# Signal of high-energy phonons created by low-energy phonons in superfluid helium

I. N. Adamenko,[1] K. E. Nemchenko,[1] V. A. Slipko,[1] and A. F. G. Wyatt[2]
[1]*Karazin Kharkov National University, Svobody Square 4, Kharkov 61077, Ukraine*
[2]*School of Physics, University of Exeter, Exeter EX4 4QL, United Kingdom*
(Received 5 December 2003; published 30 April 2004)

Starting from the solution of the kinetic equation, we have calculated the distribution function for the high-energy phonons, which are created by a short pulse of low-energy phonons moving in superfluid helium. This enables an explicit expression for the energy density flux to be derived. Hence we find the amplitude of the high-energy phonon signal as a function of time on a bolometer. We divide this signal into two halves: the ''head'' and ''tail'' which arrive before and after the peak signal, respectively. We analyze which high-energy phonons form the head and tail of the signal. The half-widths of head and tail are calculated and approximate formulas which describe the shapes of them are obtained. The partial contribution of high-energy phonons, with different momenta, to the total signal at different times is determined. These results are compared with the experimental results given in the preceding paper [R. V. Vovk, C. D. H. Williams, and A. F. G. Wyatt, Phys. Rev. B **69**, 144524 (2004)].

DOI: 10.1103/PhysRevB.69.144525 PACS number(s): 67.40.Fd

## I. INTRODUCTION

In anisotropic phonon systems, unlike isotropic ones, the phonon number density in momentum space is different in different directions. Such strongly anisotropic phonon systems are created in superfluid $^4$He at such low temperatures that the thermal excitations can be neglected (see, for example, Refs. 1–3). The heater injects phonons into this extremely pure and isotropic superfluid liquid (''a superfluid vacuum'') and these phonons move in a direction mostly normal to the surface of the heater. In momentum space, all the injected phonons are inside a narrow cone with solid angle $\Omega_p \ll 1$. This strongly anisotropic system, created near the heater, forms a phonon pulse with the dimensions in coordinate space determined by size of the heater and the duration of the heat pulse applied to the heater. This phonon pulse moves from the heater to the bolometer, which detects the temporal dependence of the incoming signal.

The interest of experimentators and theoreticians in strongly anisotropic systems is due to the unique phenomena caused by the anisotropy. These phenomena are governed by the unusual relaxation of phonons in superfluid $^4$He, which is due to the energy-momentum dependence of the phonons:

$$\varepsilon_p = cp[1+\Psi(p)], \tag{1}$$

where $c$ is the sound velocity, and $\Psi(p)$ is the function that describes the deviation from a linear dependence. Although this deviation is found to be small $[\Psi(p) \ll 1]$, it explains the type of phonon interactions found in superfluid helium.

At momentum less than the critical one $p_c$, the function $\Psi(p<p_c)>0$ and the dispersion law allows phonon processes where one phonon can decay into two or more phonons, or two or more phonons can create one phonon. In superfluid helium at saturated vapor pressure $cp_c/k = 10$ K. The rate $\nu_{3pp}$ of three-phonon processes $(3pp)$ was calculated in the limiting cases in Refs. 4 and 5, and in the general case in Ref. 6. The $3pp$ is the most rapid process which does not conserve phonon number.

At momenta $p>p_c$ the function $\Psi(p>p_c)<0$ and three-phonon processes are prohibited. As a result, the fastest processes for these phonons with high energy, are the four-phonon processes $(4pp)$, where the number of phonons in the initial and the final states is equal to two. The rate of four-phonon processes in superfluid helium $\nu_{4pp}$ was calculated in Refs. 7–9. According to the results of these calculations, which agree with the experimental data,

$$\nu_{3pp} \gg \nu_{4pp}. \tag{2}$$

Because of this inequality, phonons in superfluid helium form two subsystems with very different relaxation times: (1) The subsystem of low-energy phonons ($l$ phonons) with $p < p_c$, where equilibrium is attained very quickly; (2) the subsystem of high-energy phonons ($h$ phonons) with $p \geqslant p_c$ which take a longer time to attain equilibrium.

Under the conditions of all the known experiments, where the properties of strongly anisotropic phonon systems have been studied, the $l$ phonons attain equilibrium instantaneously. But the time to establish equilibrium in the $h$-phonon system can be comparable with and even greater than the typical times of the experiments.

The presence of two phonon systems, with quite different relaxation times, results in many unique physical phenomena which have been observed in experiments. So, in Refs. 10 and 11, experimental results were presented which showed that $h$ phonons were created by a pulse of $l$ phonon. The explanation of this phenomenon, where the cold $l$-phonon pulse, with the typical temperature $T=1$ K, is able to create $h$ phonons with energy of $\varepsilon \geqslant \varepsilon_c = 10$ K an order of magnitude greater than the temperature of $l$-phonon pulse, was given in Refs. 12–14.

The created $h$ phonons are lost from the main pulse, through the back wall, and create a second strongly anisotropic system. As a result, the single phonon pulse that is formed near the heater, creates two phonon signals by the time it reaches the bolometer, with very different temporal dependences. New experiments[1] have managed to extract the

 

temporal dependence of *h*-phonon signal, and study many properties of this unusual signal. In this paper, we consider theoretically the creation of *h* phonons by low-energy phonons in superfluid helium.

## II. THE DISTRIBUTION FUNCTION OF *h* PHONONS CREATED BY *l*-PHONON PULSE

We start by considering a pulse of low-energy phonons (*l* phonons) propagating in the liquid helium. It is created by the heater at $z=0$ and at time $t=0$ and moves along the $z$ axis. The coordinates of the back and front surfaces of the pulse are

$$z_{back}(t=0)=0, \quad z_{front}(t=0)=L. \tag{3}$$

The *l* phonons are in equilibrium and have a Bose-Einstein distribution with temperature $T_0$. However, they only occupy a narrow cone in momentum space with solid angle $\Omega_p$. So it is a very anisotropic system. The *l*-phonon pulse moves with velocity $c=238$ m/s and does not disperse.[15] The *l*-phonons interact through three phonon processes which are very fast and maintain the equilibrium on a time scale of $10^{-10}$ s. There are, however, other phonon scattering processes, the most important of which are four-phonon processes ($4pp$), which create high-energy phonons (*h* phonons). These phonons have energy $\epsilon \geqslant 10$ K and their creation rate $\nu_{b1}$ is much lower than the $3pp$ rate so we can always consider the *l* phonons to be in equilibrium. The *h* phonons have a lower group velocity than the *l*-phonons ($v_p \leqslant 189$ m/s), and so they are left behind by the *l*-phonon pulse. This loss of *h* phonons by the pulse lowers their density in the pulse below their equilibrium value at temperature *T*, so more *h* phonons are created in an attempt to restore equilibrium. Hence *h* phonons are continuously created within the pulse and then go into the *h*-phonon cloud which trails behind the *l* phonons.

The density profile of this *h*-phonon cloud is determined by their creation rate as the *l*-phonon cloud moves from the heater to the detector, at $z=z_B$, and also by their considerable dispersion. The $4pp$ creation rate is strongly dependent on *T* so as the *l*-phonon pulse cools, the number of *h* phonons created drops rapidly. The main aim of this paper is to calculate the signal shape of the *h*-phonon cloud and then compare it with experiment.[1]

The creation of *h* phonons inside the *l*-phonon pulse and their evolution in the ''superfluid vacuum'' formed by superfluid helium is described by the kinetic equation,

$$\frac{\partial n}{\partial t}+\mathbf{v}_p\frac{\partial n}{\partial \mathbf{r}}=N_b-N_d, \tag{4}$$

where $n=n(\mathbf{p},\mathbf{r},t)$ is the distribution function of *h* phonons, which determines the number of *h* phonons in the phase volume $(2\pi\hbar)^3$ that includes the phase point $\mathbf{p}$, $\mathbf{r}$ and $\mathbf{v}_p$ is the group velocity of the *h* phonons. $N_b$ and $N_d$ are the rates of increase and decrease respectively, of the occupation number of *h* phonons due to four-phonon processes.

The *h*-phonon creation rate depends on the temperature of *l* phonons, which changes with the time. The pulse cools due to the transformation of *l* phonons to *h* phonons and also due the increase of the transverse size of the *l* phonon pulse which decreases the energy density of the *l* phonons.

The results of Ref. 15 show that the transverse expansion of the pulse causes a mesa shaped energy density up to a distance $\sim 5$ mm from the heater. So, the temperature in the region along the axis of the pulse and near its center, which mainly determines the phonon flux on the bolometer that is situated on the axis of the pulse, does not change within this distance. In Ref. 15, the widening of the *l*-phonon pulse was described without taking into account *h*-phonon creation. However, there is no reason to consider that creation of *h* phonons changes the velocity of expansion of the *l* phonon pulse. So, at a distance of 5 mm, where most of the physics has happened and the important features of the *h* phonon pulse are determined, the expansion of the *l* phonon pulse can be neglected. Moreover, from the results of Ref. 16 where mesa-shaped pulses were observed at the detector, the creation of *h*-phonons results in an increase in the width of the hot spot. Thus it is reasonable to neglect the effects of transverse widening if we just consider processes near the center of the pulse, i.e., along the axis of symmetry, perpendicular to the heater. Apart from this, we neglect the lateral expansion of the pulse in this paper.

We therefore seek a one-dimensional solution to the problem of the shape of the *h*-phonon density along the $z$ axis. This approximation is valid because phonons in the pulse occupy narrow solid angle $\Omega_p \ll 1$ in momentum space.[11]

We restrict our consideration to very short pulses, for which

$$L \ll (c-v_p)\tau_d, \tag{5}$$

where $\tau_d$ is the life time of *h* phonons inside the pulse of *l* phonons. When this inequality (5) is satisfied, the *h* phonons leave the *l*-phonon pulse before they begin to interact with other *h* or *l* phonons. We also neglect interactions between *h* phonons outside the *l*-phonon pulse. This is reasonable if their density is low enough which it is if the initial temperature of the *l* phonons is not too high.

With the inequality (5) and for not too high temperature pulses, the *h* phonons have a very long lifetime and so we can put $N_d=0$ in the kinetic equation (4). Then, for the one dimensional problem, we can rewrite Eq. (4) as follows:

$$\frac{\partial n(p,z,t)}{\partial t}+v_p\frac{\partial n(p,z,t)}{\partial z}=N_b. \tag{6}$$

The solution of this equation with the initial conditions

$$n(p,z,t=0)=0 \tag{7}$$

is as follows

$$n(p,z,t)=\int_0^t N_b(p,z-v_p(t-t'),t')dt'. \tag{8}$$

This result has a simple physical meaning. The signal at point $z$ and time $t$ is formed by phonons with momentum $p$ and group velocity $v_p$, which were created at time $t'$ at the point

$$z_b = z - v_p(t - t'). \tag{9}$$

Taking into account that the *l*-phonon pulse moves with velocity $c$, the function $N_b$ in Eq. (8) can be rewritten as follows:

$$N_b(p, z_b, t') = N_{b1}(p, T(t'))\,\eta(z_b - ct')\,\eta(L - z_b + ct'), \tag{10}$$

where $\eta$ is the Heaviside step function, which is equal to unity when its argument is positive, and equal to zero when its argument is negative; $T(t')$ is the temperature of the *l*-phonon pulse.

Substituting Eq. (10) in Eq. (8) with the condition (9) gives

$$n(p,z,t) = \int_0^t N_{b1}(p, T(t'))\,\eta(z - v_p(t - t') - ct')\,\eta(L - z + v_p(t - t') + ct')dt'. \tag{11}$$

The product of the $\eta$ functions in Eq. (11) differs from zero when the time $t'$ of the *h*-phonon creation satisfies the inequality

$$\frac{z - v_p t - L}{c - v_p} \leqslant t' \leqslant \frac{z - v_p t}{c - v_p}. \tag{12}$$

According to this inequality the interval $\delta t'$ is equal to

$$\delta t' = \frac{L}{c - v_p}. \tag{13}$$

In short pulses, when the inequality (5) is valid, during the time interval (13), the temperature of the *l* phonons in the pulse, essentially does not change. In this case the function $N_{b1}(p, T(t'))$ can be taken out of the integral with the value of $t'$ equal to right-hand side (rhs) of inequality (12) we thus obtain the distribution function for the *h* phonons,

$$n(p,z,t) = \frac{L}{c - v_p} N_{b1}(p, T(t_b))\,\eta(t - t_b)\,\eta(t_b), \tag{14}$$

where

$$t_b = \frac{z - v_p t}{c - v_p}. \tag{15}$$

This time has a simple physical meaning. This is the time the *h*-phonons, with momentum $p$, are created, after which they move ballistically with velocity $v_p$ and reach point $z$ at time $t$. The expression (15) can be obtained also from Eq. (9), putting $t' = t_b$ and taking into account that

$$z_b = c t_b \tag{16}$$

since the pulse moves with the velocity $c$ for time $t_b$ to point $z_b$.

According to Refs. 12–14,

$$N_{b1}(p,T) = n_p^{(0)} \nu_{b1}(p,T), \tag{17}$$

where $\nu_{b1}$ is the rate of creation of *h* phonon inside the main pulse of *l* phonons and

$$n_p^{(0)} = (e^{\varepsilon_p / kT} - 1)^{-1} \tag{18}$$

is the Bose-Einstein distribution function for *h* phonons.

In Ref. 17 $\nu_{b1}(p,T)$ was calculated and showed that this rate decreases as $p$ increases from $p_c$. For all the problems solved earlier, because of the exponential dependence on $\varepsilon_p$ in Eq. (17) the main contribution was due to phonons with momentum close to $p_c$. So, the momentum dependence has little influence on the earlier results Refs. 12, 13, and 14. In the problem solved here, the shape of the *h*-phonon signal is determined by a considerable range of momenta $p$. Thus, it is important to carry out exact calculations with the momentum and temperature dependence for $\nu_{b1}(p,T)$ (see Ref. 9).

The rate $\nu_{b1}(p,T)$ given in Refs. 17 and 9 can be presented with sufficient accuracy by the following expression:

$$\nu_{b1}(p,T) = A_1 e^{-A_2/T} e^{-A_3[c(p - p_c)/k]}, \tag{19}$$

where $A_1 = 1.228 \times 10^9\ \mathrm{s}^{-1}$, $A_2 = 3.188\ \mathrm{K}$, and $A_3 = 1.65\ \mathrm{K}^{-1}$.

The dependence $T = T(t_b)$ can be found using conservation of energy; the energy going to the creation of *h* phonons comes from the *l* phonons. So, for a short enough pulse, when we can neglect the second term in the right-hand side (rhs) of Eq. (4), we get the rate of change of the *l*-phonon energy density (see Refs. 12–14)

$$\frac{\partial E_l^{(0)}}{\partial t_b} = -E_h^{(0)} \overline{\nu_{b1}}, \tag{20}$$

where

$$E_l^{(0)} = \frac{\Omega_p \pi k^4 T^4}{120 \hbar^3 c^3} \tag{21}$$

is the energy density of *l* phonons with Bose-Einstein distribution function,

$$E_h^{(0)} = \frac{\Omega_p k^4 T \varepsilon_c^3 e^{-\varepsilon_c / T}}{(2\pi\hbar)^3 c^2 v_c} \tag{22}$$

is the energy density of *h* phonons with distribution function (18), $v_c$ is the group velocity of *h* phonons with momentum $p = p_c$, and

$$\overline{\nu_{b1}(T)} = \frac{1}{E_h^{(0)}} \int \varepsilon n_p^{(0)} \nu_{b1} \frac{d^3 p}{(2\pi\hbar)^3} \tag{23}$$

is the average value of the *h*-phonon creation rate $\nu_{b1} = \nu_{b1}(\mathbf{p}, T)$.

At present, the creation rates have only been calculated for *h* phonons which move along the z axis (see Ref. 17). So, to obtain analytical expressions we assume that the rate $\nu_{b1}$ is given by Eq. (19) for all *h* phonons, created in the solid angle $\Omega_p$ and is equal to zero for those *h* phonons with momenta lying outside the solid angle $\Omega_p$. Taking into account this assumption, we obtain from Eqs. (19) and (23),

$$\overline{\nu_{b1}(T)} = A_1 e^{-A_2/T} \left(1 + A_3 \frac{c}{v_c} T\right)^{-1}. \tag{24}$$

Substituting Eqs. (21), (22), and (24) in formula (20) we get the equation for the function $T(t_b)$, the solution of which, with initial condition

$$T(t_b=0)=T_0 \tag{25}$$

can be presented in the following form:

$$\frac{\overline{\nu_{b1}(T)}}{T^4}e^{-\varepsilon_c/T}=\frac{\overline{\nu_{b1}(T_0)}}{T_0^4}e^{-\varepsilon_c/T_0}\left(1+\frac{t_b}{\tau_S}\right)^{-1}, \tag{26}$$

where

$$\tau_S=\frac{4E_l^{(0)}(T_0)}{E_h^{(0)}(T_0)\,\overline{\nu_{b1}(T_0)}}\frac{T_0}{\varepsilon_c+A_2}. \tag{27}$$

While deriving result (26) we have taken into account that $\varepsilon_c \gg T_0$.

By substituting of Eqs. (17) and (19) in Eq. (14) we obtain an explicit expression for the *h*-phonon distribution function created by *l*-phonon pulse

$$n(p,z,t)=\frac{LA_1}{c-v_p}n_p^{(0)}e^{-A_2/T(t_b)}e^{-A_3[c(p-p_c)/k]}\eta(t-t_b)\,\eta(t_b), \tag{28}$$

where the function $T(t_b)$ is determined by relations (26), (27), and function $t_b=t_b(p,z,t)$ is given by Eq. (15). The result (28) solves the given problem; it gives us the number of created *h* phonons with momentum *p* in any spatial point *z* and at an arbitrary time moment *t*.

## III. TEMPORAL DEPENDENCE OF THE *h*-PHONON SIGNAL

The amplitude of the *h*-phonon signal at the bolomoter is determined by the energy density flux through unit area of the surface at $z=z_B$, which is perpendicular to axis *z*. This energy density flux is given by the following equation:

$$I(t)=\int_{p_c}^{p_{max}} v_p\varepsilon_p n(p,z_B,t)\frac{\Omega_p p^2 dp}{(2\pi\hbar)^3}. \tag{29}$$

Here $p_{max}$ is the maximum momentum of the phonons which we consider. We take

$$\frac{cp_{max}}{k}=14\,\mathrm{K}; \tag{30}$$

as higher-momentum phonons contribute very little. The group velocity $v_p$ can be well approximated by the expression

$$v_p=v_c-\alpha\frac{c(p-p_c)}{k}, \tag{31}$$

where $v_c=189\ \mathrm{m\,s^{-1}}$, and $\alpha=18.5\ \mathrm{m\,s^{-1}\,K^{-1}}$.

Substitution of Eq. (28) to Eq. (29) gives

$$I(t)=\frac{\Omega_p LA_1}{(2\pi\hbar)^3}\int_{p_c}^{p_{max}}\frac{v_p\varepsilon_p p^2}{c-v_p}e^{-(\varepsilon_p+kA_2)/kT(t_B)}\times e^{-A_3[c(p-p_c)/k]}\eta\left(t-\frac{z_B}{c}\right)\eta\left(\frac{z_B}{v_p}-t\right)dp, \tag{32}$$

where, in accordance with Eq. (15),

$$t_B=\frac{z_B-v_p t}{c-v_p} \tag{33}$$

is the time of creation of *h* phonon with momentum *p* which reaches the bolometer at time *t*. The function $T(t_B)$ is determined by Eq. (26) by changing $t_b$ to $t_B$. In expression (32) we simplified the function (18) due to the strong inequality $\varepsilon_c/T \gg 1$.

Relation (32) completely determines the temporal dependence of the energy density flux at the point $z_B$, where the bolometer is situated. This dependence will be discussed before Eq. (32) is integrated.

The integrand in Eq. (32) gives the contribution from the *h* phonons with momentum *p* in the interval $dp$, to the energy flux on the bolometer at time *t*. We identify this energy flux with the measured signal.

From Eq. (32) it follows that signal starts at time $t_{st}$,

$$t_{st}=\frac{z_B}{c}, \tag{34}$$

when both $\eta$ functions in Eq. (32) are equal to unity. At time (34), according to Eq. (33), the signal is due to *h*-phonon created time,

$$t_B(t_{st})=t_{st}, \tag{35}$$

i.e., when the *l*-phonon pulse reaches the detector. At this time (35) the temperature of *l* phonons has its minimum value due to the creation of *h* phonon as the *l*-phonon pulse travels from the heater to the detector. The minimum temperature *T*, according to Eqs. (17) and (19), results in a minimum partial contribution for all momenta in expression (32) at time $t=t_{st}$.

At later detection times, after $t_{st}$, the creation time of the *h* phonon, $t_B$, decreases according to Eq. (33) from its maximum value (35) to zero , and the temperature of *l*-phonons, according to Eq. (26), increases. The increase in temperature with the increase of *t*, defined in Eq. (33), and the decrease in $t_B$ according to Eq. (32), results in a monotonic increase of all the partial contributions to the signal (see Fig. 1) up to its maximum value. We see from Eq. (32) that the largest partial contributions come from phonons with the least momentum, i.e., $p=p_c$.

The partial signal reaches its maximum value at time

$$t_{end}(p)=\frac{z_B}{v_p} \tag{36}$$

when the second $\eta$ function in Eq. (32) still is equal to unity. According to Eq. (33) at time $t_{end}$, Eq. (36), the detected *h* phonons were created at time

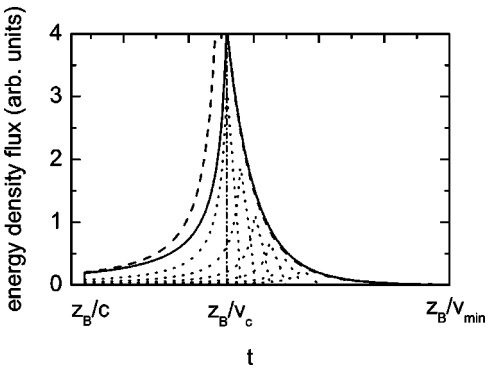


FIG. 1. The temporal dependence of the *h*-phonon energy density flux (amplitude of the *h*-phonon signal on the bolometer), obtained by Eq. (32), at point $z=z_B$ (solid line) and partial contributions (dotted lines) of six serial regions of momenta in intervals $p_c+(n-1)\Delta p<p<p_c+n\Delta p$, where $n=1$–6, and $c\Delta p/k=0.2$ K. Dashed lines represent the approximate expressions for the "head" (48) and the "tail" (57) of the pulse. The initial temperature of *l*-phonon pulse is $T_0=1$ K and $z_B=10$ mm.

$$t_B(t=t_{end})=0, \tag{37}$$

i.e., just in front of the heater, where the temperature of *l* phonons is highest. This explains why the maximum partial contribution of all phonons occurs at times (36) (see Fig. 1).

At times

$$t>t_{end}(p) \tag{38}$$

the second $\eta$ function becomes equal to zero and phonons with momentum *p*, for which this inequality is valid do not contribute to the signal.

According to Eq. (31) the group velocity of phonons decreases as their momentum increases. This is why the maximum contribution from phonons with momentum *p* occurs at later times as *p* increases (see Fig. 1). At times

$$t>t_{end}(p_{max})=\frac{z_B}{v_{min}} \tag{39}$$

the signal is equal to zero, as all phonons (even those with the largest momentum which we have taken to be 14 K for practical purposes, which have the slowest group velocity $v_{min}=115\ \mathrm{m\,s^{-1}}$) have reached the detector. According to Eq. (32), the maximum partial contribution from phonons with $p=p_{max}$ is 1/730 of that for phonons with $p=p_c$. Also from expression (32), it follows that the maximum value of the partial amplitude is greatest for phonons with momentum $p=p_c$ and monotonically decreases with momentum reaching its minimum value at $p=p_{max}$.

The full signal is obtained by integration of all the partial contributions. From the arguments above, the full signal reaches its maximum value at time

$$t_{end}(p_c)=\frac{z_B}{v_c}. \tag{40}$$

This can be seen in Fig. 1, and the same result follows from Eq. (32).

The temporal dependence of the energy density flux (the integrated signal) shown in Fig. 1 can be separated into two parts: the "head" of the pulse, when amplitude grows from zero to its maximum value, and the "tail" of the pulse, when the amplitude decreases from its maximum to zero with time. The head of the pulse is detected during the time interval

$$\frac{z_B}{c}\leqslant t\leqslant\frac{z_B}{v_c}, \tag{41}$$

and the tail—during the time interval

$$\frac{z_B}{v_c}\leqslant t\leqslant\frac{z_B}{v_{min}}. \tag{42}$$

The head of the pulse is formed by phonons with momentum close to $p_c$, which are created almost over the whole propagation path of the *l*-phonon pulse from the heater to the detector. The tail consists of phonons with $p>p_c$ which are created over part of the path starting at the heater. This partial path depends on the momentum of the phonon and is defined by the inequality

$$0\leqslant z\leqslant z_B\frac{v_c-v_p}{c-v_p}\frac{c}{v_c}. \tag{43}$$

This can be understood as the maximum value of *z* is given by the requirement that a phonon created at this point, with group velocity $v_p$, arrives at the detector at time $z_B/v_c$, which is the start of the tail. Phonons with $v_p$ created nearer the heater will arrive later, and those created at the heater give the lower bound in the inequality. The r.h.s. of inequality (43) has a maximum value for the slowest phonons, i.e., those with $v_p=v_{min}$, which is at a distance of $0.757z_B$. So we see that the tail is formed from phonons created at large distances from the heater but their contribution is small.

The result (28) allows us to find a partial contribution of *h* phonons with given momentum *p* to the amplitude of the signal on the bolometer (see Fig. 1) at any time moment. Figure 2 for $T_0=1$K and $z_B=10$ mm presents the momentum dependence of the relative phonon number density

$$n(p,z_B,t)p^2/n(p_c,z_B,t_{end}(p_c))p_c^2, \tag{44}$$

in accordance with Eq. (28) for three times.

(1) The time $t=t_{end}(p_c)-\tau_{head}$ corresponding to the half-width of the head (curve 1).

(2) The time $t=t_{end}(p_c)$ corresponding to the maximum (see Fig. 1) of the signal (curve 2).

(3) The time $t=t_{end}(p_c)+\tau_{tail}$ corresponding to the half-width of the tail (curve 3).

The momentum dependence of the relative phonon number integrated over time

$$\int_{z_B/c}^{z_B/v_{min}} n(p,z_B,t)p^2dt \Big/ \int_{z_B/c}^{z_B/v_{min}} n(p_c,z_B,t)p_c^2dt \tag{45}$$

is described by curve 4.

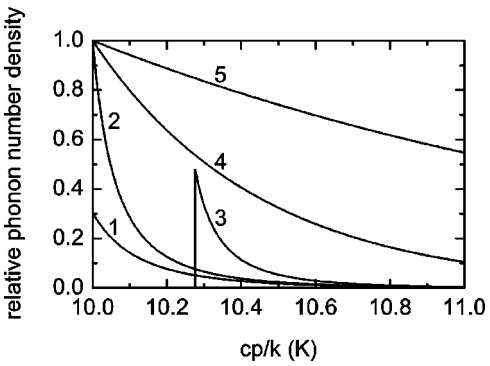


FIG. 2. The dependence of the relative phonon number density, obtained by Eqs. (28) and (44), on the momentum $p$ at the time moments corresponding to the half-width of the ''head'' (curve 1), the maximum (curve 2), and the half-width of the ''tail'' (curve 3) of $h$-phonon signal on bolometer $z_B=10$ mm at initial temperature $l$-phonon pulse $T_0=1$ K. The momentum dependence of the relative phonon number density integrated over time, obtained by Eqs. (28) and (45), is shown in curve 4. Curve 5 shows the dependence on the momentum p of the relative phonon number density (46) for a Bose-Einstein distribution function at $T=1$ K for comparison.

For comparison the momentum dependence of the relative phonon number density of Bose-Einstein (18) distribution function

$$n_p^{(0)}p^2/n_{p_c}^{(0)}p_c^2 \tag{46}$$

is described by curve 5.

The steeper slope of curves 1, 2, 3 in Fig. 2 compared with curve 5, can be explained by the presence in the r.h.s. of Eq. (28), of not only $n_p^{(0)}$, but also the second exponent.

Note that the information about partial contribution of $h$ phonons with given momentum $p$ to the signal on bolometer is important for describing quantum evaporation phenomena.

## IV. THE SHAPE OF THE HEAD AND THE TAIL OF THE *h*-PHONON SIGNAL

The head of the $h$-phonon signal is mostly due to phonons with momentum close to $p_c$, which were created at different times (33). The region in the vicinity of the maximum at $t \leqslant z_B/v_c$ is formed by phonons created near the heater, when the temperature of $l$-phonons is close to the initial temperature $T_0$. These phonons determine the maximum value of the amplitude at $t=z_B/v_c$ $(t_B=0)$. When time decreases from the value $z_B/v_c$ (and $t_B$ increases from zero) the amplitude of the signal begins to decrease according to Eq. (32) and (26).

The half-width of the head, $\tau_{head}$, can be estimated as its value is proportional to the half-width of the function $N_{b1}(p,T(t_B))$, which, according to Eqs. (14) and (29), determines the amplitude of the signal, taken at the point $p=p_c$. For an estimate of the half-width of $N_{b1}(p,T(t_B))|_{p=p_c}$ we can take that for the left-hand side of Eq. (26), it is equal to $\tau_S$. Finally, according to Eq. (33) the half-width of the head approximately is given by equality

$$\tau_{head}=\frac{c-v_c}{v_c}\tau_S. \tag{47}$$

According to Eqs. (47) and (27) an increase in $T_0$ causes $\tau_{head}$ to decrease due to the rapid decrease of $\tau_S$, and so the sharpness of the head increases with $T_0$.

From relation (32) one can obtain an approximate formula which qualitatively describes the shape of the head of the $h$-phonon signal (see Fig. 1). For this purpose it is sufficient to substitute $p$ with its typical values $p_c$ in Eq. (32), and find the region of integration of Eq. (32) from the exponential terms in the integrand in Eq. (32).

The result for the time interval (41) is

$$I(t)=\frac{\Omega_p L}{(2\pi\hbar)^3}\frac{p_c^2\varepsilon_c v_c}{c-v_c}A_1 \times\exp\left(-\frac{A_2+\varepsilon_c}{T(t_{Bc})}\right)\frac{k}{c}\left(A_3+\frac{v_c}{cT(t_{Bc})}\right)^{-1}, \tag{48}$$

where

$$t_{Bc}=\frac{z_B-v_c t}{c-v_c}.$$

The tail of $h$-phonon signal at the moment of time $t$ is formed by phonons with momentum $p\geqslant p_{min}(t)$, where $p_{min}(t)$ is the momentum which makes the argument of the second $\eta$ function in integral (32) equal to zero. Using this condition for the half-width of the tail of the pulse we obtain the following expression.

$$\tau_{tail}=\frac{z_B}{v_{p_c+\Delta p}}-\frac{z_B}{v_c}\approx\frac{z_B}{v_c^2}\left|\frac{\partial v_p}{\partial p}\right|_{p=p_c}\Delta p, \tag{49}$$

where $\Delta p$ is the typical interval of momentum change, which according to Eq. (32), can be equal to

$$\Delta p=\frac{k}{c}\left(A_3+\frac{v_c}{cT_0}\right)^{-1}. \tag{50}$$

According to the relations (49) and (50) the half-width of the tail unlike the halfwidth of the head [see Eqs. (47) and (49)], only weakly depends on temperature $T_0$.

From relation (32) it is possible to obtain the approximate formula which describes the shape of the tail when $t \geqslant z_B/v_c$. In this case the expression (32) can be rewritten in the following form:

$$I(t)=\frac{\Omega_p L A_1}{(2\pi\hbar)^3}\int_{p_{min}}^{p_{max}}\frac{v_p\varepsilon_p p^2}{c-v_p}e^{-(\varepsilon_p+kA_2)/kT(t_B)} \times e^{-A_3[c(p-p_c)/k]}dp, \tag{51}$$

where $v_{p_{\min}}=z_B/t$ and $t\geqslant z_B/v_c$. By using the relation (31) and the definition of $v_{p_{\min}}$ we obtain

$$p_{\min}=p_c+\frac{k}{\alpha c}\left(v_c-\frac{z_B}{t}\right). \tag{52}$$

The exponential dependence of the function under integration in Eq. (51) allows us to replace $p$ by $p_{\min}$ in the weakly varying preexponential factor, to expand $\varepsilon_p$ to an accuracy which is linear with respect to the $(p-p_c)$ term in the first exponent and to consider the upper limit in the integral (51) to be equal to infinity. In the expression, obtained in this way, we introduce a new variable $p'$ by the equality

$$p = p' + p_{\min} - p_c . \tag{53}$$

As a result the approximated expression for Eq. (51) can be presented in the following form:

$$I(t) = \frac{\Omega_p L A_1}{(2\pi\hbar)^3} \frac{v_{p_{min}} \varepsilon_{p_{min}} p_{min}^2}{c - v_{p_{min}}} \int_{p_c}^{\infty} e^{-(\varepsilon_c + A_2)/T(t_B)} \times e^{-(A_3 + v_c/cT(t_B))[c(p'-p_c)/k]} \times e^{-(A_3 + v_c/cT(t_B))[c(p_{min}-p_c)/k]} dp' . \tag{54}$$

Because of the weak dependence upon temperature in the third exponent of Eq. (54) we can substitute $T(t_B)$ by $T_0$ since the ''tail'' of the signal is formed essentially by phonons created near the heater, when $T \approx T_0$. In the other exponent, we should take into account that $T = T(t_B)$, where, in accordance with Eqs. (33) and (53),

$$t_B = t_B(t, p = p' + p_{min} - p_c). \tag{55}$$

Since the momentum interval, which gives the main contribution to the integral (54), is small in comparison with $p_c$, we can approximate the function (55) as follows:

$$t_B \approx t_B(t = z_B/v_c, p = p'). \tag{56}$$

Starting from Eq. (54) and using the approximations made above, we express the density of the energy flux at any time $t \geqslant z_B/v_c$, through its maximum value $I(t = z_B/v_c)$,

$$I(t) = \frac{v_{p_{min}} \varepsilon_{p_{min}} p_{min}^2}{v_c \varepsilon_c p_c^2} \frac{c - v_c}{c - v_{p_{min}}} e^{-(A_3 + v_c/cT_0)(v_c - z_B/t)(1/\alpha)} \times I\left(t = \frac{z_B}{v_c}\right), \tag{57}$$

where $p_{min}$ is determined by Eq. (52)

The dashed line in Fig. 1 calculated using Eq. (57), almost coincides with the solid line corresponded to the exact formula (51) for the shape of the tail.

The result (57) allows to investigate analytically in detail the shape of the tail. We see that the shape of the tail depends weakly on the initial temperature $T_0$. The half-width of the tail, obtained from the condition that the energy flux density, Eq. (57), has decreased to $e^{-1}$ of its peak value, reproduces the result (49), (50). According to Eq. (57) the tail of the *h*-phonon signal exists only because of the dispersion of the *h* phonons. For decreasing dispersion, $(\alpha \to 0)$ the r.h.s. of Eq. (57) decreases exponentially. If dispersion is absent ($\alpha = 0$) then the tail disappears, i.e., the signal ends at $t = z_B/v_c$ immediately after its maximum value.

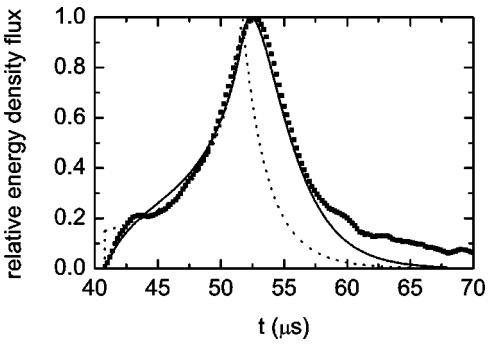


FIG. 3. Temporal dependencies, obtained by Eqs. (32) and (58), of normalized averaged (solid line) and not averaged (dotted line) densities of energy flux of *h* phonons at $z_B = 10$ mm, $\tau_B = 1.8$ $\mu$s, and initial temperature of *l*-phonon pulse $T_0 = 0.86$ K. The squares denote the normalized experimental data from Ref. 1 of a measured *h*-phonon signal with heat pulse length $t_p = 50$ ns and power $W = 6.25$ mW/mm$^2$.

To compare the signal calculated by Eq. (32) with experimental data, it is necessary to take into account the finite value of the time constant, $\tau_B$, of the detector. The detector cannot respond to very sharp signals; essentially it averages the energy density flux over the finite time interval $\tau_B$.

This average value of *h*-phonon signal is given by

$$\overline{I(t)} = \int_0^{\infty} I(t - t') e^{-t'/\tau_B} \frac{dt'}{\tau_B}. \tag{58}$$

The time constant of the bolometer $\tau_B$ was chosen to make the time of the maximum of the experimental curve and calculated curve coincide, hence $\tau_B = 1.8$ $\mu$s. In Fig. 3 the experimental data is compared with that given by Eq. (58).

It can be seen in Fig. 3 that the averaged curve given by Eq. (58) changes more slowly than the curve calculated directly from Eq. (32). This difference is caused by the integration, with the finite value of the time constant, which smoothes out very sharp variations on the temporal scale $\tau_B$. Here we should note that the maxima of the exact and averaged curves occur at different times. The averaged curve peaks later by $\approx \tau_B$.

At present there are experimental data for the different lengths of the heat pulses at various powers.[1] However, the theory presented here is only applicable for short pulses, satisfying the inequality (5), and for low powers so that any interaction between *h* phonons can be neglected. Here we should note that at the values chosen for Fig. 3 $T_0 = 0.86$ K and $t_p = 50$ ns the inequality (5) is strong. However, at $T_0 = 1$ K and $t_p = 50$ ns this inequality becomes not so strong. Figure 3 shows that there is agreement between the calculated averaged energy density flux and the measured signal up to the time $t = 58$ $\mu$s. The comparatively large experimental value of the signal at $t > 58$ $\mu$s is thought to be an artifact of the bolometer.[1]

## V. CONCLUSION

Starting from the solution of the kinetic equation (4), the distribution function (28) is obtained that gives the number density of *h* phonons, as a function of momentum, at any spatial and temporal points which are created by a short pulse of *l* phonons.

The solution (28) allows us to write an explicit expression (32) for the density of the energy flux, which determines the amplitude of *h*-phonon signal on the bolometer, situated at the point $z=z_B$.

From the expression (32) it follows that the temporal dependence of the energy density flux (the signal as a function of time on the bolometer) can be separated on two parts (see Fig. 1): the head of the pulse, where amplitude grows from zero to its maximum value, and the tail, where amplitude decreases from maximum to zero.

The expression (32) allows us to analyze which *h* phonons form the head and the tail, to find the half-widths of the head (47), and tail (49), and to obtain approximate expressions which describe the shape of the head (48) and tail (57) (see the dashed lines in Fig. 1).

Starting from the result (28), the partial contribution of the *h* phonons, with a given momentum, to the amplitude of the signal on the bolometer as a function of time is found. The time-integrated values of the partial contributions (see Fig. 2) are also found.

The experimental data, on the temporal dependence of relative signal amplitude, are compared with the values calculated by formulas (32) and (58) (see Fig. 3). The calculated signal agrees well with the measured one up to time $t=58$ $\mu$s. For $t>58$ $\mu$s the measured signal differs from that calculated. However, it is suggested in the preceding paper, Ref. 1, that the relatively large measured signal at $t>58$ $\mu$s is probably an artifact.

The theory developed in this paper has some restrictions which made the problem tractable. Let us consider these simplifications.

(1) Only short *l*-phonon pulses were considered, for which the inequality (5) is valid. In this case one can omit the second term, in the r.h.s. of the kinetic equation (4), which describes processes of *h*-phonon decay inside the main pulse of *l* phonons.

(2) It was supposed that initial temperature of the main *l*-phonon pulse is relatively low. This allows us to neglect interactions between the created *h* phonons, during their motion to the bolometer.

(3) We neglected the lateral expansion of the *l*-phonon pulse. The justification for this approximation can be found in Refs. 15 and 16, where it was shown that a hot spot can exist for a long time along the axis of the pulse.

(4) We have found a one-dimensional solution of the problem, in which all *h*-phonons propagate parallel to axis *z*. The evidence for such an approximation is given by the results of Ref. 11 according to which, phonons in the pulse occupy a very narrow solid angle in momentum space.

All the above-mentioned restrictions do not prevent one from understanding the physics of the phenomenon of creation of *h* phonons, and getting agreement between the calculated shape of the *h*-phonon signal and the measured signal, for a short pulse and relatively low heating power.

We note that an unusual phenomenon was observed in heat pulses created in solids at low temperatures.[18,19] In Ref. 19 it was shown that heat pulses created in solids may be self-trapped if nonlinear effects and dispersion are taken into account. This phenomenon was observed in Ref. 18 only for pulses of transverse phonons under high input power. The possibility of a self-trapping effect in helium needs special consideration. Here we should note that in the experiments of Ref. 1, the maximum input power was at least two orders of magnitude less than the input power at which the effect of self-trapping was observed in Ref. 18. Moreover, there are no transverse phonons in helium. Furthermore, the self-trapping effect observed in Ref. 18 has a temporal scale of about 0.5 $\mu$s, but in the experiments in Ref. 1 the time constant of the bolometer is of about 1.5 $\mu$s.

The theory developed in this paper explains a number of observed phenomena for short and low power pulses. Among these phenomena one can point to the observed linear dependence of the *h*-phonon pulse height on pulse length (see Fig. 4 in Ref. 1) for relatively short pulses, and the increase of the half-width of the head of the signal with decreasing input power (see Fig. 7 in Ref. 1) for relatively low powers.

However, many interesting phenomena observed in Ref. 1 at high input power and longer pulse lengths cannot be described by the theory presented here. This gives us an impetus to further develop the theory.

## ACKNOWLEDGMENTS

We express our gratitude to EPSRC of the UK (Grant Nos. GR/S24855 and GR/N20225), and to GFFI of Ukraine (Grant No. 2.07/000372) for support for this work.

[1] R.V. Vovk, C.D.H. Williams, and A.F.G. Wyatt, preceding paper, Phys. Rev. B **69**, 144524 (2004).
[2] A.F.G. Wyatt, N.A. Lockerbie, and R.A. Sherlock, Phys. Rev. Lett. **33**, 1425 (1974).
[3] F.R. Hope, M.J. Baird, and A.F.G. Wyatt, Phys. Rev. Lett. **52**, 1528 (1984).
[4] C. Havlin and M. Luban, Phys. Lett. **42A**, 133 (1967).
[5] H.J. Maris, Phys. Rev. A **9**, 1412 (1974).
[6] M.A.H. Tucker, A.F.G. Wyatt, I.N. Adamenko, K.E. Nemchenko, and A.V. Zhukov, Fiz. Nizk. Temp. **25**, 657 (1999) [J. Low Temp. Phys. **25**, 488 (1999)].
[7] M.A.H. Tucker and A.F.G. Wyatt, J. Phys.: Condens. Matter **4**, 7745 (1992).
[8] I.N. Adamenko, K.E. Nemchenko, and A.F.G. Wyatt, J. Low Temp. Phys. **126**, 1471 (2002).
[9] I.N. Adamenko, Y.A. Kitsenko, K.E. Nemchenko, V.A. Slipko,

and A.F.G. Wyatt (unpublished).
[10] M.A.H. Tucker and A.F.G. Wyatt, J. Phys.: Condens. Matter **6**, 2813 (1994).
[11] M.A.H. Tucker and A.F.G. Wyatt, J. Phys.: Condens. Matter **6**, 2825 (1994).
[12] I.N. Adamenko, K.E. Nemchenko, A.V. Zhukov, M.A.H. Tucker, and A.F.G. Wyatt, Phys. Rev. Lett. **82**, 1482 (1999).
[13] A.F.G. Wyatt, M.A.H. Tucker, I.N. Adamenko, K.E. Nemchenko, and A.V. Zhukov, Phys. Rev. B **62**, 9402 (2000).
[14] I.N. Adamenko, K.E. Nemchenko, and A.F.G. Wyatt, Fiz. Nizk. Temp. **28**, 123 (2002) [J. Low Temp. Phys. **28**, 85 (2002)].
[15] I.N. Adamenko, K.E. Nemchenko, V.A. Slipko, and A.F.G. Wyatt, Phys. Rev. B **68**, 134507 (2003).
[16] R.V. Vovk, C.D.H. Williams, and A.F.G. Wyatt, Phys. Rev. B **68**, 134508 (2003).
[17] I.N. Adamenko, K.E. Nemchenko, and A.F.G. Wyatt, J. Low Temp. Phys. **125**, 1 (2001).
[18] V. Narayamamurti and C.M. Varma, Phys. Rev. Lett. **25**, 1105 (1970).
[19] F.D. Tappert and C.M. Varma, Phys. Rev. Lett. **25**, 1425 (1970).